Enhanced nonlinear Cherenkov radiation on the crystal boundary

Huaijin Ren,[1] Xuewei Deng,[2,4] Yuanlin Zheng,[1] Ning An,[1] and Xianfeng Chen[1,3]

[1]*Department of Physics, Key Laboratory for Laser Plasmas (Ministry of Education) Shanghai Jiao Tong University, 800 Dongchuan Road, Shanghai 200240, China*

[2]*Laser Fusion Research Center, China Academy of Engineering Physics, Mianyang, Sichuan 621900, China*

[3]*e-mail: xfchen@sjtu.edu.cn*

[4]*e-mail: xwdeng@caep.ac.cn*

Received March 25, 2013; revised May 8, 2013; accepted May 10, 2013;
posted May 13, 2013 (Doc. ID 187620); published May 31, 2013

We demonstrate a method to generate enhanced nonlinear Cherenkov radiation (NCR) in the bulk medium by utilizing the total reflection on the physical boundaries inside the crystal. This is the experimental demonstration of enhanced NCR by a sharp $\chi^{(2)}$ modulation from 0 to 1, and a new way for generating enhanced NCR in addition to using the waveguide structures and the ferroelectric domain walls, which also possesses a better beam quality for applications.

OCIS codes: (190.0190) Nonlinear optics; (190.2620) Harmonic generation and mixing; (190.4350) Nonlinear optics at surfaces.

http://dx.doi.org/10.1364/OL.38.001993

Nonlinear Cherenkov radiation (NCR), which is an auto-phase-matched second harmonic (SH) generation process, was discovered in the early days of nonlinear optics [1] and used to generate high-efficiency SHs in waveguide structures [2–4]. With the development of nonlinear optics and materials, researchers found that the NCR could be significantly enhanced in materials with multiple ferroelectric domains [4–7]. Precise lateral scanning also reveals that enhanced NCR existed in the vicinity of ferroelectric domain walls [8,9]. This could be explained by two main reasons: First, the new enhanced elements of susceptibility tensor in domain wall resulting from lattice distortion or internal local electrical field by poling process [8]; and second, arbitrary reciprocal vectors provided by the antiparallel domains across the domain wall [10], which could compensate for the phase mismatch in the nonlinear optical process. Besides Cherenkov SH generation, many other Cherenkov-type nonlinear processes have been found, including sum frequency generation [11,12], third and higher order harmonic generation [13,14], difference frequency generation [15], and so on. Since NCR is a noncollinear auto-phase-matched frequency conversion process and is quite sensitive to the ferroelectric domain wall, it has been utilized as an effective tool for nondestructive diagnostics, microscopy [16] and ultrashort pulse characterization [12].

In bulk medium, the conversion efficiency of NCR is so low that it is not suitable for practical applications. Till now, only waveguide structures and ferroelectric domain walls have been demonstrated to be valid for efficient NCR. Different from the automatic phase matching of fundamental mode and radiated harmonic mode in waveguide structures, enhanced NCR in domain walls results from the sharp −1 to 1 $\chi^{(2)}$ modulation across domain wall [10]. According to previous theoretical studies, such sharp $\chi^{(2)}$ modulation constitutes a sufficient condition for the emission of NCR. However, such domain walls with −1 to 1 $\chi^{(2)}$ modulation are artificial structures, involving uncertain factors such as lattice distortion and local electrical field, which may cause beam quality degradation. Theoretically, sharp $\chi^{(2)}$ modulation from 1 to 0, such as the boundary of nonlinear crystal, can also cause the enhanced NCR [10], but there is still not much research reported.

In this Letter, we demonstrate experimentally that the physical boundaries of a nonlinear crystal can be used to generate enhanced NCR, by utilizing the sum frequency polarization along these boundaries in the condition of total internal reflection. Since the polished crystal surface does not involve complex artificial structures, it can provide excellent beam quality, which means a higher precision in diagnostics and microscopy.

The most basic condition for NCR is $v_p > v_2$ or $k_p < k_2$, meaning the phase velocity of nonlinear polarization wave exceeds that of harmonic waves in the nonlinear medium. When total internal reflection occurs on the crystal boundary, as shown in Fig. 1(a), the incident light and the reflected light stimulate a sum frequency polarization wave, which can be expressed as

$$P^{\mathrm{NL}} = 4\varepsilon_0 d_{\mathrm{eff}} E_1^2 e^{i[(\vec{k}_1+\vec{k}_1')\cdot\vec{r}-2\omega t]}, \tag{1}$$

where $\vec{k}_1$, $\vec{k}_1'$ are the wave vector of the incident light and reflected light, respectively. The wave vector of sum frequency polarization wave is $\vec{k}_p = \vec{k}_1 + \vec{k}_1'$, which propagates along the direction of the reflecting interface and with the value of $k_p = 2k_1 \cos\alpha$, supposing the incident angle is α. It should be noted that birefringent crystals under certain conditions may display the characteristics of anomalous dispersion, i.e., the refractive index of the harmonics is less than that of the fundamental when they are with different polarization [17]. As shown in Figs. 1(b) and 1(c), in normal dispersion situation, NCR generated by sum frequency polarization wave begins with a very small incident angle; while in anomalous dispersion situation, only when the incident angle is large enough to satisfy $k_p < k_2$, is NCR possible to appear.

In the experiments, we used a sample of 5%/mol MgO:$LiNbO_3$ crystal with dimensions of 3 mm × 20 mm ×

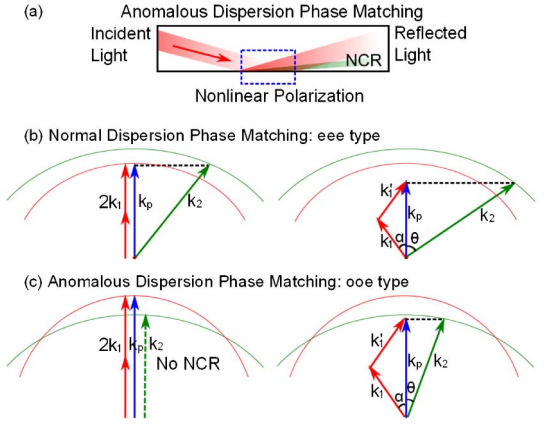

Fig. 1. (a) Through total internal reflection on the crystal boundary, NCR can be produced by the sum frequency polarization wave. (b) and (c) Phase-matching geometries of different dispersion situations with normal and oblique incidence.

2 mm ($x \times y \times z$). The sample was laid on a rotation stage, so that the incident angle could be freely adjusted in the x–z plane, as shown in Fig. 2(a). The laser source was a femtosecond optical parametric amplifier (TOPAS, Coherent Inc.) with a repetition rate of 1000 Hz. After adjustment of the polarization state by the combined reflecting mirrors, the laser beam was loosely focused into the sample by a 250 mm focal lens.

At first, the sample was illuminated along x axis with the vertically polarized laser beam at the center wavelength of 1190 nm. In this case, there was no NCR, which was in agreement with the phase-matching relation in Fig. 1(c). What we could observe was just a phase-mismatched collinear SH beam, and a conical SH beam caused by the scattering light. For oblique incidence, we adjusted the crystal's position so that the fundamental beam could be reflected on the crystal boundary. When the incident angle was slightly greater than the critical condition $\alpha = \arccos(k_2/2k_1)$, NCR gradually emerged from short wavelength to long wavelength, as shown in Fig. 2(b). The light spot on the left of NCR in the photograph is a phase mismatched collinear SH generated by the reflected light, and there is also a spot on the other side of the symmetrical position originated from multiple reflections. As we continued to increase the incident angle, the Cherenkov radiation angle also became larger; Figs. 2(b)–2(d) display this process.

Now we analyze the role of the crystal boundary in the experiment. First of all, NCR is indeed produced by the single reflection in the vicinity of the crystal boundary, but not by the overlapping of the multiple reflected lights in the middle of the crystal. In general, NCR in bulk medium presents a circular ring pattern [18], but we observed a NCR spot with obvious dispersion along the vertical direction of the reflection interface (x–y plane). NCR possessing this feature must be generated by planar-structure-like periodically poled lithium niobate (PPLN) or single domain wall. The difference is that there was only one bright sum frequency NCR in this experiment, rather than a symmetrical pattern on both sides of domain wall. In fact, the other spot disappeared due to total reflection, which is further evidence that NCR was generated at the boundary. When the fundamental beam illuminated on the y face of the sample, it could reflect twice since the crystal dimension along the y axis was longer, and there were two NCR spots derived from two boundaries. The result is shown in Fig. 3(a). Second, crystal boundary does not only provide a mechanism to change phase-matching condition by the reflection angle, but has an effect on the enhancement of NCR. Here the enhancement is relative to the NCR inside bulk medium. In order to demonstrate this, we did a comparative experiment by exploiting the extraordinary-polarized fundamental beam for ee-e-type nonlinear process. Under normal dispersion condition, SH polarization wave generated by the incident light itself can meet the phase matching condition of $k_p < k_2$ [Fig. 1(b)]. But NCR was still not observed unless the incident light encountered the crystal boundary. Similarly, when we divided the incident light into two beams and made them overlap within the crystal, the Cherenkov sum frequency also could not be produced. These both indicate that the boundary region plays an important role in the enhancement of NCR.

Compared to the enhanced NCR in domain walls which results from the sharp −1 to 1 $\chi^{(2)}$ modulation, NCR generated at the boundaries of the crystal has very good beam quality. Figure 3(b) shows the NCR generated by an A-grade 5%/mol MgO:PPLN sample. As we can see, the spatial intensity distribution of NCR generated at the boundary is relatively smooth while NCR generated from PPLN has an obvious periodic modulation. These modulations may be derived from the spectral interference caused by the periodic structure of PPLN, or result from nonuniform distribution of the refractive index and second-order nonlinear coefficient near the domain wall.

We measured the emergence angle and the relative intensity of NCR depending on the incident angle of fundamental beam at wavelength of 1135 nm at the room

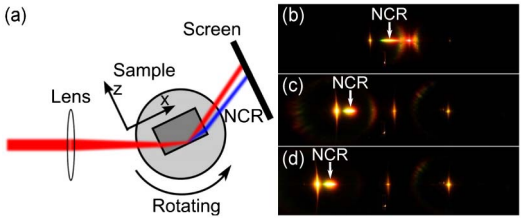

Fig. 2. (a) Schematic of the experimental setup. (b)–(d) Photographs of NCR with different incident angles.

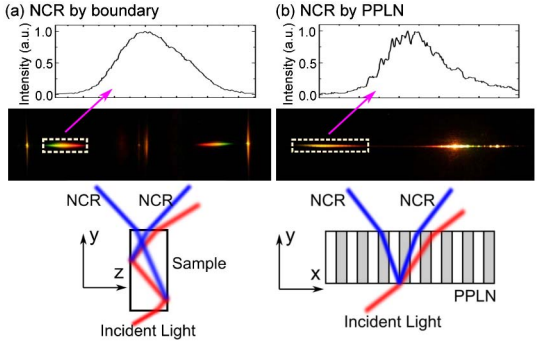

Fig. 3. Comparison of NCR from the bulk crystal boundary and from PPLN.

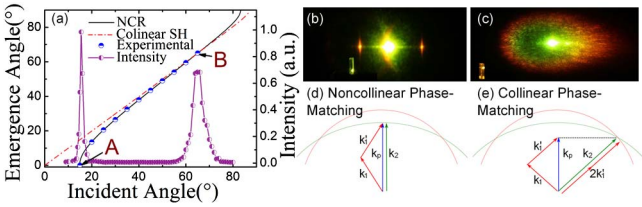

Fig. 4. (a) External emergence angle of NCR and collinear SH as a function of the external incident angle. (b) The bright spot in the middle is degenerated NCR [point A in (a)]. (c) NCR and collinear SH overlap [point B in (a)]. The color ring on the periphery is conical SH caused by scattering light of lower-frequency components. (d) and (e) are the corresponding phase-matching geometries of (b) and (c), respectively.

temperature of 20°C. According to Fig. 1(c), the oo-e-type phase-matching relationship between the Cherenkov angle θ and the incident angle α inside the crystal satisfies $n_{1o}\cos\alpha = n_{2e}(\theta)\cos\theta$, which can be further written as

$$n_{1o}\cos\alpha = \frac{n_{2e}n_{2o}}{\sqrt{n_{2o}^2 + n_{2e}^2 tg^2\theta}}. \quad (2)$$

Figure 4(a) displays the experimental results and the theoretical calculation of NCR emergence angle (black solid line), as well as the emergence angle of SH beam collinear with the reflected light (red dashed–dotted line). There are two specific points, i.e., point A with the NCR emergence angle of 0° and point B where the curves of NCR emergence angle and collinear SH emergence angle intersect. Figures 4(b) and 4(c) show the experimental photos of the light spots at points A and B. Based on the enhancement by sharp $\chi^{(2)}$ modulation from 1 to 0 of the crystal boundary, the output intensity was further enhanced by about two orders of magnitude at these two points.

Actually, point A corresponds to the NCR degenerate state which satisfies the critical Cherenkov condition $2k_1\cos\alpha = k_2$. Previous research has suggested that NCR degenerate state cannot be observed in domain wall, because the opposite nonlinear coefficients on different sides of the domain wall lead to destructive interference [17], but this problem does not exist on the crystal boundary. The reason for its enhancement can be figured out by the matching relationship in Fig. 4(d). At this time, the wave vector of the incident light, the reflected light, and the harmonic constitute a triangular complete phase-matching. Point B is another critical situation. After going through this point, the position of NCR will be changed from the inside of the collinear SH to the outside. As shown in Fig. 4(e), point B also corresponds to the intersection of the refractive index ellipse of the fundamental ordinary light and the extraordinary harmonic light, where the reflected light and the harmonic satisfy the collinear complete phase-matching condition $2k_1 = k_2$. From the above analysis, we can see that generally the NCR only meets the longitudinal phase-matching conditions, but in these two specific cases complete phase-matching can be achieved, resulting in the enhancement of a certain frequency component.

In summary, we experimentally demonstrated that the sum frequency polarization wave generated by total reflection on the crystal boundary can produce enhanced NCR. This is a new method to generate NCR on the interface with 0–1 abrupt change of nonlinear coefficient, in addition to the waveguide and the domain wall structure. At two specific incident angles, the NCR had a high conversion efficiency because of narrowband complete phase matching. Compared to NCR in optical superlattice materials, NCR on the crystal boundary has better beam quality and greater potential for application.

This work was supported in part by the National Basic Research Program 973 of China under Grant 2011CB-808101, the National Natural Science Foundation of China under Grants 61125503, 61235009, and 61205110, the Foundation for Development of Science and Technology of Shanghai under Grant 11XD1402600, and in part by the Innovative Foundation of Laser Fusion Research Center.

References

1. A. Zembrod, H. Puell, and J. A. Giordmaine, Opt. Quantum Electron. **1**, 64 (1969).
2. P. K. Tien, R. Ulrich, and R. J. Martin, Appl. Phys. Lett. **17**, 447 (1970).
3. M. J. Li, M. de Micheli, Q. He, and D. B. Ostrowsky, IEEE J. Quantum Electron. **26**, 1384 (1990).
4. Y. Zhang, Z. D. Gao, Z. Qi, S. N. Zhu, and N. B. Ming, Phys. Rev. Lett. **100**, 163904 (2008).
5. A. R. Tunyagi, M. Ulex, and K. Betzler, Phys. Rev. Lett. **90**, 243901 (2003).
6. S. M. Saltiel, D. N. Neshev, R. Fischer, W. Krolikowski, A. Arie, and Y. S. Kivshar, Phys. Rev. Lett. **100**, 103902 (2008).
7. S. M. Saltiel, D. N. Neshev, W. Krolikowski, A. Arie, O. Bang, and Y. S. Kivshar, Opt. Lett. **34**, 848 (2009).
8. A. Fragemann, V. Pasiskevicius, and F. Laurell, Appl. Phys. Lett. **85**, 375 (2004).
9. X. W. Deng, H. J. Ren, H. Y. Lao, and X. F. Chen, J. Opt. Soc. Am. B **27**, 1475 (2010).
10. Y. Sheng, V. Roppo, K. Kalinowski, and W. Krolikowski, Opt. Lett. **37**, 3864 (2012).
11. S. M. Saltiel, D. N. Neshev, W. Krolikowski, N. Voloch-Bloch, A. Arie, O. Bang, and Y. S. Kivshar, Phys. Rev. Lett. **104**, 083902 (2010).
12. A. S. Aleksandrovsky, A. M. Vyunishev, A. I. Zaitsev, A. A. Ikonnikov, and G. I. Pospelov, Appl. Phys. Lett. **98**, 061104 (2011).
13. Y. Sheng, W. J. Wang, R. Shiloh, V. Roppo, Y. F. Kong, A. Arie, and W. Krolikowski, Appl. Phys. Lett. **98**, 241114 (2011).
14. N. An, H. J. Ren, Y. L. Zheng, X. W. Deng, and X. F. Chen, Appl. Phys. Lett. **100**, 221103 (2012).
15. C. Chen, X. Hu, Y. Xu, P. Xu, G. Zhao, and S. Zhu, Appl. Phys. Lett. **101**, 071113 (2012).
16. X. W. Deng and X. F. Chen, Opt. Express **18**, 15597 (2010).
17. H. Ren, X. Deng, Y. Zheng, N. An, and X. Chen, Phys. Rev. Lett. **108**, 223901 (2012).
18. V. Vaičaitis, Opt. Commun. **209**, 485 (2002).